

# RSC Advances



This is an *Accepted Manuscript*, which has been through the Royal Society of Chemistry peer review process and has been accepted for publication.

*Accepted Manuscripts* are published online shortly after acceptance, before technical editing, formatting and proof reading. Using this free service, authors can make their results available to the community, in citable form, before we publish the edited article. This *Accepted Manuscript* will be replaced by the edited, formatted and paginated article as soon as this is available.

You can find more information about *Accepted Manuscripts* in the [Information for Authors](#).

Please note that technical editing may introduce minor changes to the text and/or graphics, which may alter content. The journal's standard [Terms & Conditions](#) and the [Ethical guidelines](#) still apply. In no event shall the Royal Society of Chemistry be held responsible for any errors or omissions in this *Accepted Manuscript* or any consequences arising from the use of any information it contains.

1 **Preparation and characterization of expanded perlite/paraffin composite with enhanced**  
2 **thermal conductivity and leakage-bearing properties by graphene oxide**

3

4 *Zeyu LU<sup>1</sup>, Dongshuai HOU<sup>2,\*</sup>, Biwan XU<sup>1</sup>, Zongjin LI<sup>1</sup>*

5 *1. Department of Civil and Environmental Engineering, The Hong Kong University of Science and*  
6 *Technology, Hong Kong, China.*

7 *2. Department of Civil Engineering, Qingdao Technological University (Cooperative Innovation Center*  
8 *of Engineering Construction and Safety in Shandong Blue Economic Zone), Qingdao, China*

9 *Tel.: +852-9162-6614; Fax: +852-2358-1534.*

10 *\* Corresponding author: Dongshuai HOU; E-mail: dhou@ust.hk;*

11

12

**Abstract**

13 A novel phase change materials (PCMs) of expanded perlite/paraffin/graphene oxide  
14 (EP/PA/GO) with enhanced thermal conductivity and leakage-bearing properties was fabricated  
15 by depositing GO films on the surface of the EP/PA composite. The as-prepared EP/PA/GO  
16 composite was characterized by using Differential scanning calorimetry (DSC),  
17 Thermogravimetric analysis (TGA), Fourier transform infrared spectroscopy (FTIR) and  
18 Scanning electron microscopy (SEM) techniques. The experimental results indicated that due to  
19 the small loading of the GO incorporation within 0.5 wt.%, the EP/PA/GO composite showed a  
20 small latent heat capacity and weight loss, and the thermal conductivity significantly increased  
21 with increasing content of GO up to 0.5 wt. %. The heat storage/release performance test results  
22 demonstrated that the EP/PA composite with 0.5 wt. % GO had 2 times faster heat  
23 storage/release rate compared to the EP/PA composite because of the enhanced thermal  
24 conductivity. In addition, the FTIR and TGA results indicated that the EP/PA/GO composite had  
25 a good chemical compatibility and thermal stability. More importantly, the GO films covering the  
26 surface of the EP/PA composite can greatly prevent the leakage problems of the molten paraffin.  
27 No leakage of paraffin occurred even after thermal cycling 3000 times. Therefore, the EP/PA/GO  
28 composite has a great potential for thermal energy storage applications due to its enhanced  
29 thermal properties, good leakage-bearing properties and excellent chemical compatibility.

30

31 *Keywords:* phase change materials; graphene oxide; thermal conductivity; leakage-bearing  
32 properties.

33

## 34 **1. Introduction**

35 Latent thermal energy storage (LTES) is a promising approach to improve solar energy  
36 utilization and minimize energy dissipation in buildings due to its high energy storage density  
37 and capacity at constant temperature [1, 2]. Phase change materials (PCMs) are widely used in  
38 the LTES system and have been receiving great attention for various applications in solar heating  
39 systems, building energy conservation and air-conditioning systems [1, 3-5]. PCMs mainly  
40 include inorganic PCMs such as alloys, melted salts and crystalline hydrated salts, and organic  
41 PCMs such as paraffin, fatty acids/esters and lauric acid [6, 7]. However, the leakage problem  
42 after melting and the lower thermal conductivity of PCMs are the two main drawbacks limiting  
43 wide application. One way to prevent the leakage problem is by using micro- and macro-  
44 encapsulation methods, including interfacial polymerisation, emulsion polymerization and situ  
45 polymerization [8, 9]. PCMs form the core with a polymer shell to maintain the shape and  
46 protect the PCMs from leakage. However, the aging, cost and lower thermal conductivity of  
47 encapsulation shells have been the biggest concern for this method. The other way is to  
48 impregnate PCMs into porous materials, such as diatomite [10, 11] and expanded perlite [7, 12].  
49 Lu et al.[13, 14] have fabricated a form-stable expanded perlite/paraffin (EP/PA) composite by  
50 absorbing paraffin into porous networks of expanded perlite, resulting in good thermal energy  
51 storage, thermal stability and thermal reliability. The leakage problem can be resolved to some  
52 extent by the capillary and surface tension forces of porous materials [15, 16]. However, the  
53 lower thermal conductivity of porous materials reduces the heat transfer rate, which has a  
54 negative effect on the energy storage efficiency of PCMs composites. Thus far, much research  
55 has been done to mix PCMs composites with graphite-based materials, due to excellent thermal  
56 conductivity, such as graphite, expanded graphite and carbon nanotubes (CNTs). Tian et al. [17]  
57 investigated shaped-stabilized PCMs composites of ternary eutectic chloride/ expanded graphite  
58 (EG), and revealed that the thermal conductivities of the composites were 1.35–1.78 times higher  
59 than that of the pure ternary eutectic chloride. Mhike et al. [18] attempted to improve the thermal  
60 conductivity of PCMs composites by adding graphite and EG. It was found that 10 wt. %  
61 graphite and EG showed increases of 60 % and 200 % in thermal conductivity of the PCMs

62 composites, respectively. However, the higher content of graphite reduces the phase change  
63 enthalpy of PCMs composites, and the particle-like graphite has no contribution to preventing  
64 the leakage problems of the PCMs composites. In addition, Xu et al. [19] have shown that the  
65 use of 0.26% MWCNTs can bring clear beneficial effects in improving the thermal conductivity  
66 and heat storage/ release rates of the PCMs composites without influencing the chemical  
67 compatibility and thermal stability. However, it is still difficult to disperse CNTs uniformly in  
68 PCMs composites due to the high surface energy and hydrophobic properties. Therefore, it is  
69 very important and urgent to develop an improved method, not only encapsulating the PCMs  
70 composites, but also improving the thermal conductivity of the PCMs composites.

71  
72 Graphene oxide (GO) is a two-dimensional single layer material with  $sp^2$ -bonded carbon atoms,  
73 decorated by a large number of covalent oxygen-containing groups-hydroxyl, carbonyl and  
74 carboxyl [20]. The exceptional mechanical and thermal properties of GO make it a good  
75 candidate for a wide range of applications, such as polymer composite materials, energy storage,  
76 biomedical applications and catalysis [21, 22]. It is well known that graphene is a perfect  
77 membrane that can completely block the penetration of molecules [23]. Although defects are  
78 introduced into the GO structures due to the strong oxidation process, the permeability and  
79 thermal conductivity of the GO greatly depends on the oxidation degree and the numbers of  
80 layers of the GO. To the best of our knowledge, the well-controlled GO is generally thought to  
81 be a perfect material that can prevent the leakage of viscous PCMs and improve the thermal  
82 conductivity of the PCMs composites.

83  
84 In this study, paraffin and expanded perlite were selected to prepare a EP/PA composite with a  
85 high latent heat and a suitable melting temperature for use in buildings, and the GO coating was  
86 deposited on the surface of the EP/PA composite. The as-prepared EP/PA/GO composite was  
87 composed of paraffin as the core, expanded perlite as the supporting material, and the GO films  
88 as the exterior shell. The oxidation degree and the thickness of the GO films deposited on the  
89 surface of the EP/PA/GO composite were investigated by X-ray photoelectron spectroscopy  
90 (XPS) and typical optical microscopy. The thermal performance of the EP/PA/GO composite was  
91 characterized by differential scanning calorimeter (DSC) analysis, thermogravimetric (TGA)  
92 analysis and heat storage/release performance tests. The morphology of the EP/PA/GO

93 composite was observed by using a scanning electron microscope (SEM). Chemical  
94 compatibility between the paraffin, expanded perlite and GO, was measured by using Fourier  
95 transform infrared spectroscopy (FTIR) analysis. The leakage-bearing properties of the  
96 EP/PA/GO composite were investigated by a traditional and a newly designed leakage test.

97

## 98 **2. Experimental**

### 99 **2.1 Materials**

100 Paraffin in technical grade was supplied by the Ke Qitai Chemical Company, Guangzhou, China.  
101 The density and thermal conductivity of the paraffin were  $0.81 \text{ g/cm}^3$  and  $0.21 \text{ W/m}\cdot\text{ }^\circ\text{C}$ ,  
102 respectively. Expanded perlite was obtained from the Zhongde Perlite Factory, Liaoning, China.  
103 The density and mean grain size of the expanded perlite used were  $0.31 \text{ g/cm}^3$  and 2-3 mm,  
104 respectively. Graphite powder (200 mesh, 99.9995 %, *metal basis*) was purchased from Alfa  
105 Aesar Inc, Tianjin, China.

106

### 107 **2.2 Preparation of the GO**

108 GO was prepared from graphite powder (Alfa-Aesar, 200 mesh) according to the modified  
109 Hummers' method [24]. Graphite powder (3 g) was added to a solution containing  $\text{K}_2\text{S}_2\text{O}_8$  (2 g),  
110  $\text{P}_2\text{O}_5$  (2 g) and concentrated  $\text{H}_2\text{SO}_4$  (40 mL, 98 wt. %) for 6 h mixing at  $80 \text{ }^\circ\text{C}$ . The resulting  
111 mixture was then diluted with distilled water, filtered and washed until the pH value of the rinse  
112 water became neutral. The dried graphite oxide was re-dispersed into concentrated  $\text{H}_2\text{SO}_4$  (100  
113 mL, 98 wt. %) in an ice bath.  $\text{KMnO}_4$  (15 g) was gradually added and stirred for 2 h. The  
114 mixture was then stirred and mixed at  $35 \text{ }^\circ\text{C}$  for another 2 h, followed by the addition of 230 mL  
115 of distilled water. The resultant bright yellow solution was terminated by adding 700 mL of  
116 distilled water and 15 mL 30%  $\text{H}_2\text{O}_2$ , and subjected to centrifugation and careful washing by  
117 37 % HCl and distilled water. After immersing the as-prepared suspension in dialysis tubing  
118 cellulose membranes for 7 days, it was finally centrifuged and collected for preparing different  
119 concentrations of graphene oxide solution. In this study, the concentration of the GO solution  
120 was  $2.0 \text{ mg/mL}$ .

121

### 122 **2.3 Preparation of the EP/PA/GO composite**

123 The form-stable EP/PA composite was prepared in the following steps. The mass fraction of  
124 paraffin in the EP/PA composite was 0.55 because the homogenous EP/PA composite can be  
125 obtained by the direct impregnation method based on our previous research [13]. Firstly, paraffin  
126 was melted at a temperature of  $50\text{ }^{\circ}\text{C} \pm 5\text{ }^{\circ}\text{C}$  for 1 h in an oven, and then immediately mixed with  
127 expanded perlite at ambient temperature and put back in the oven. The mixture was mixed every  
128 hour until the paraffin was uniformly dispersed in the expanded perlite. Finally, the form-stable  
129 EP/PA composite was formed after cooling down at room temperature. Then, the as-prepared  
130 EP/PA composites were added into the GO solution (2 mg/mL) and magnetically stirred for 30  
131 min to ensure a uniform dispersion. The resultant mixture was poured into a glass beaker and put  
132 into an oven at a temperature of  $80\text{ }^{\circ}\text{C} \pm 5\text{ }^{\circ}\text{C}$  for 3 hours. The EP/PA/GO composites were  
133 finally fabricated after completing GO solvent evaporation. The color of the as-prepared  
134 EP/PA/GO composite changed from white to black due to the successful GO deposition onto the  
135 surface of the EP/PA composite, as shown in Fig. 1. The mass fractions of GO in the EP/PA/GO  
136 composite were 0.25 wt. % and 0.5 wt. %, and referred to as EP/PA/GO0.25 and EP/PA/GO0.5,  
137 respectively.

138

### 139 **2.4 Characterization**

140 The oxidation degree and the thickness of the GO films were determined by XPS analysis (5600  
141 multi-technique system, Physical Electronics) and typical optical microscopy (BX51, Olympus).  
142 The thermal performances of the EP/PA/GO composite were characterized by DSC analysis  
143 (TAQ 1000) with a heating and cooling rate of  $5\text{ }^{\circ}\text{C min}$  under a nitrogen atmosphere. The  
144 thermal conductivity the EP/PA/GO composite was verified by comparing the heat  
145 storage/release rates of the EP/PA composite with that of the EP/PA/GO composite. The thermal  
146 stability of the EP/PA/GO composite was studied by the TGA method (Perkin Elmer) at  $10\text{ }^{\circ}\text{C}$   
147 /min under a nitrogen environment. The morphology of the EP/PA/GO composite was observed  
148 by using SEM (JEOL, JEM-6390). Chemical compatibility between paraffin, expanded perlite  
149 and GO, was measured by FTIR analysis (Bio-Rad FTS 6000). The leakage-bearing properties of  
150 the EP/PA/GO composite were investigated by a traditional and a newly designed leakage test.

151

### 152 3. Results and discussion

#### 153 3.1 DSC analysis of the EP/PA/GO composite

154 Fig. 2 shows the DSC curves of the EP/PA composite with different GO contents. The detailed  
 155 thermal results of the measured latent heat ( $H_M$ ) and the peak phase change temperature ( $T_{peak}$ )  
 156 are listed in Table 1. As presented in Fig. 2 and Table 1, the value of  $T_{peak}$  in the melting and  
 157 freezing processes were determined as 50.72 °C and 42.54 °C for the EP/PA composite, and  
 158 50.86 °C and 42.22 °C for the EP/PA/GO0.25 composite, and 50.96 °C and 42.14 °C for the  
 159 EP/PA/GO0.5 composite. The results indicate that the GO incorporation does not cause a shift of  
 160 the peak phase change temperature of the EP/PA composite. Moreover, the value of  $H_M$  in the  
 161 melting and freezing processes were 80.92 J/g and 80.48 J/g for the EP/PA composite, 80.16 J/g  
 162 and 80.21 J/g for the EP/PA/GO0.25 composite and 79.75 J/g and 79.36 J/g for the EP/PA/GO0.5  
 163 composite. It clearly can be seen that the EP/PA composite, with and without the GO, shows an  
 164 almost equivalent latent heat capacity and low latent heat capacity loss resulting from the small  
 165 loading of GO incorporation, within 0.5 wt. %. Therefore, it can be concluded that 0.5 wt. % GO  
 166 leads to a trivial change of the values of  $H_M$  and  $T_{peak}$  of the EP/PA composite, and that the  
 167 EP/PA/GO composite can be effectively used as an energy storage material for exterior walls in  
 168 building applications.

169  
 170 **Table 1** Thermal properties of the EP/PA composite with different content of the GO.  
 171

Composite	<i>Melting Process</i>		<i>Freezing Process</i>	
	$T_{peak}$ (°C)	$H_M$ (J/g)	$T_{peak}$ (°C)	$H_M$ (J/g)
EP/PA	50.72	80.92	42.54	80.84
EP/PA/GO0.25	50.86	80.16	42.22	80.21
EP/PA/GO0.5	50.96	79.75	42.14	79.36

172

173

#### 174 3.2 Thermal stability of the EP/PA/GO composite

175 The thermal stability of the EP/PA composite with different GO contents was evaluated by TGA  
176 analysis. Fig. 3 shows the measured TGA curves of the EP/PA composite, the EP/PA/GO0.25  
177 composite and the EP/PA/GO0.5 composite. As shown in Fig. 3, the EP/PA composite starts to  
178 lose weight at approximately 105 °C. After rapid weight loss due to paraffin evaporation, there is  
179 a loss of 55.24 % of the paraffin weight at 360 °C, which is almost consistent with the design  
180 mix proportion of the expanded perlite and paraffin, indicating that the EP/PA composite is  
181 homogeneous. With the incorporation of the GO, there are no obvious changes in the starting  
182 decomposition temperature and the weight loss rate the EP/PA/GO composite. The only  
183 differences, by comparing the three curves in Fig. 3, are the final weight loss of the different  
184 composites. Compared with the weight loss of the EP/PA composite (55.24 %), it slightly  
185 increases to 55.50 % and 55.82 % for the EP/PA/GO0.25 composite and the EP/PA/GO0.5  
186 composite, respectively. The negligible change is attributed to the small GO loading, up to 0.5  
187 wt. %. In addition, no decomposition is seen for all the composites over their phase change  
188 temperature ranges, showing the good thermal stability of the EP/PA/GO composite.

189

### 190 **3.3 Thermal conductivity of the EP/PA/GO composite**

191 Thermal conductivity is a key parameter to determine the thermal storage performance of PCMs  
192 composites. The heat storage/release performance of the EP/PA/GO composite was investigated  
193 by using the test setup schematically shown in Fig. 4 [19]. In this test, 5 g of the PCMs  
194 composite was stored in a sealed tube. Two water baths, at temperatures of 60 °C and 30 °C,  
195 were adopted during the heating storage/release processes. The temperature change of the PCMs  
196 composite during the heating storage/release test was measured by thermocouples located in the  
197 middle of the PCMs composite stack in the sealed tube and recorded through a data-logger and a  
198 computer.

199

200 Fig. 5 shows the temperature curves for melting and freezing of the EP/PA composite with  
201 different GO mass fractions in the heat storage/release performance tests. Table 2 lists the time  
202 taken for temperatures increasing from 30 °C to 60 °C and decreasing from 60 °C to 30 °C. The  
203 shorter the time, the faster the heat storage and release rate, and the higher the thermal  
204 conductivity of the composite. As shown in Fig. 5 and Table 2, all the composites have obvious  
205 temperature plateaus in the heating and cooling processes due to the occurrence of phase

206 changes. In detail, when temperature increases from 30 °C to 60 °C, it takes 8.8 min, 6.2 min and  
 207 4.1 min for the EP/PA composite, the EP/PA/GO0.25 composite and the EP/PA/GO0.5,  
 208 respectively. Similarly, it takes 14.2 min, 11.8 min and 7.5 min for each composite when the  
 209 temperature decreases from 60 °C to 30 °C. It clearly shows that the time used for both the  
 210 melting and freezing processes decreases with the increasing content of GO within 0.5 wt. %,  
 211 and the EP/PA/GO0.25 and EP/PA/GO0.5 composites show clearly faster heat storage and  
 212 release rates than the EP/PA composite. The experimental results indicate that the EP/PA/GO0.5  
 213 composite has 2 times faster heat storage/release rates compared to that of the EP/PA composite  
 214 due to the enhanced thermal conductivity. The significant improvement is much better than many  
 215 other studies reported. For example, Li et al. [19] demonstrated that 0.26 wt. % CNTs led to 1.25  
 216 times faster heat storage/release rates for paraffin/diatomite composites; however, uniform  
 217 dispersion of CNTs in the PCMs composite is difficult to accomplish. Liu et al. [25] have shown  
 218 that the time required in heat storage/release tests was reduced by 3 times with the addition of 1  
 219 wt. % graphite; however, the latent heat loss of the composite decreased significantly due to the  
 220 higher loading of the graphite, and the leakage problem still could not be avoided by the addition  
 221 of graphite. In this study, 0.5 wt. % GO incorporation not only reduces the time required in heat  
 222 storage/release tests by a factor of 2, but also keeps the latent heat capacity of the PCMs  
 223 composite stable. Therefore, GO has a great influence on improving the thermal properties of the  
 224 EP/PA composite.

225  
 226 Table 2 Time for heating and cooling of EP/PA composite with different GO content

Composite	EP/PA	EP/PA/GO0.25	EP/PA/GO0.5
Temperature range			
30 °C -60 °C	8.8 min	6.2 min	4.1 min
60 °C -30 °C	14.2 min	11.8 min	7.5 min

227

### 228 3.4 Chemical compatibility of the EP/PA/GO composite

229 Fig. 6 shows the FTIR spectrums of the EP/PA composite with different GO contents. As  
 230 presented in Fig. 6, the characteristic peaks of the GO at 1723  $\text{cm}^{-1}$ , 1621  $\text{cm}^{-1}$ , 1222  $\text{cm}^{-1}$  and  
 231 1058  $\text{cm}^{-1}$  indicate carboxyl or carbonyl C=O stretching, H-O-H bending band of the absorbed  
 232 H<sub>2</sub>O molecules, phenolic C-OH stretching and alkoxy C-O stretching, respectively. Moreover,

233 the EP/PA composite has six characteristic absorption bands: skeleton vibration of C-C at 455  
234  $\text{cm}^{-1}$ , rocking vibration of  $-\text{CH}_2$  at  $718 \text{ cm}^{-1}$ , two deformation vibrations of  $-\text{CH}_2$  and  $-\text{CH}_3$  at  
235  $1368 \text{ cm}^{-1}$  and  $1468 \text{ cm}^{-1}$ , and two stretching vibrations of  $-\text{CH}_2$  and  $-\text{CH}_3$  at  $2848 \text{ cm}^{-1}$  and  $2917$   
236  $\text{cm}^{-1}$ , respectively. It is clearly seen that all the above-mentioned characteristic absorption bands  
237 of the GO and the EP/PA composite are included in the FTIR spectrums of the EP/PA/GO0.5  
238 composite. More importantly, no new characteristic absorption bands are generated in the FTIR  
239 spectrums of the EP/PA/GO0.5 composite, suggesting that there is no chemical reaction between  
240 the GO and the EP/PA composite. Therefore, it can be concluded that the EP/PA/GO composite  
241 has a good chemical compatibility.

242

### 243 3.5 Leakage-bearing properties of the EP/PA/GO composite

244 Fig. 7 shows the SEM images of the surface morphologies of the expanded perlite, the EP/PA  
245 composite and the EP/PA/GO composite. As seen from Fig. 7a, the expanded perlite has a highly  
246 porous structure, which makes it a good supporting material to absorb molten paraffin. Fig. 7b  
247 shows that the paraffin is uniformly absorbed into the pores of the expanded perlite, and hence  
248 the leakage of the molten paraffin from the composites is largely prevented. Fig. 7c shows the GO  
249 coating on the surface of the EP/PA composite. It is clear that the pores of the EP/PA composite  
250 are encapsulated with the GO coating, which acts like a shell to prevent the molten paraffin  
251 leaking out. However, whether the molten paraffin can permeate the GO coating makes a great  
252 influence on the leakage-bearing properties of the EP/PA/GO composite. In order to verify this  
253 point, leakage testing for the GO films was conducted, as shown in Fig. 8. The GO film was  
254 obtained from the GO solution (the dosage and concentration equivalent to that used for the  
255 fabrication of the EP/PA/GO0.5 composite) by an oven drying method, and then placed into the  
256 middle of the suction device (Fig. 8). The lamp was turned on to ensure that the paraffin was in a  
257 molten condition during the leakage test. The experimental results showed that there is no molten  
258 paraffin penetrated through the GO films to the bottom conical flask after 24 h heating, which  
259 confirms that the GO films are effective in preventing the leakage of the molten paraffin.  
260 Moreover, the traditional leakage test was carried under condition in which the EP/PA composite  
261 and the EP/PA/GO0.5 composite were put on a filter and placed under the lamp, as seen in Fig.  
262 9. The distance between the lamp and the composite was 10 cm to ensure that all the paraffin

263 could melt and solidify in the thermal cycling test with 3 min of lamp ‘on’ and 9 min of lamp  
264 ‘off’. The experimental results revealed that there was no paraffin trace on the filter for the  
265 EP/PA composite and the EP/PA/GO0.5 composite after 1500 thermal cycles, because the molten  
266 paraffin could be limited in the pores of the expanded perlite by the capillary and surface tension  
267 forces. However, after 3000 cycling, a small amount of paraffin was observed on the filter for the  
268 EP/PA composite, caused by the paraffin leakage, but there was no paraffin trace on the filter for  
269 the EP/PA/GO0.5 composite, as seen in Fig. 10c and 10f. The possible reason is that the GO  
270 coating on the surface of the EP/PA/GO0.5 composite contributes to preventing the molten  
271 paraffin leakage, which is consistent with the previous results as seen in Fig. 8. It also indicates  
272 that the leakage protection for the molten paraffin, caused by the capillary and surface tension  
273 forces of the expanded perlite, is good for short term use; however, the EP/PA composite covered  
274 with GO coating shows an excellent leakage-bearing property, which has great potential for use  
275 in energy efficient buildings for long term consideration.

276  
277 Since the permeability of the GO coating greatly depends on the thickness and the oxidation  
278 degree of the GO layers, the cross-section of the EP/PA/GO0.5 composite was examined by an  
279 optical microscopy to measure the thickness of the GO coating, and the XPS test was carried out  
280 to investigate the oxidation degree of the GO. Fig. 11a shows the cross-sectional image of the  
281 EP/PA/GO0.5 composite. It is clear that the surface of the composite is uniformly covered by the  
282 GO films, and the thickness of the GO films is about 50  $\mu\text{m}$ . Fig. 11b shows the XPS spectra of  
283 the GO used in this study, and the deconvoluted C1s XPS spectra of the GO, clearly shows four  
284 types of carbon bonds, including the C-C at 284.5 eV, C-O at 286.4 eV, C=O 288.3 at eV and -  
285 COOH at 289.0 eV. The elemental analysis of the XPS results indicate that the C/O ratio and  
286 oxygen content of the GO in this study are 3.0 and 30.7 %, respectively. Therefore, it can be  
287 concluded that the GO films with a C/O ratio of 3.0 and thickness of 50  $\mu\text{m}$ , in this study, can  
288 effectively prevent the leakage problem of the EP/PA composite for long term use. However, it  
289 should be noted that the leakage-bearing properties of the EP/PA/GO composite greatly depends  
290 on the oxidation degree and the thickness of the GO films. A greater oxidation degree or less  
291 thickness of the GO films might cause negative effects on the leakage-bearing properties of the  
292 EP/PA/GO composite.

293

#### 294 4. Conclusions

295 In this study, a novel phase change material of expanded perlite/paraffin/graphene oxide  
296 (EP/PA/GO) with enhanced thermal properties was fabricated by depositing GO films on the  
297 surface of the EP/PA composite. The DSC and TGA results showed that the EP/PA/GO  
298 composites had small latent heat capacity and weight losses due to the small loading of the GO  
299 incorporation, within 0.5 wt. %. The FTIR results indicated that the EP/PA/GO composite had  
300 good chemical compatibility. In addition, due to the excellent thermal conductivity of the GO,  
301 the heat storage/release performance test results showed that the EP/PA/GO0.5 composite had 2  
302 times faster heat storage/release rates compared to that of the EP/PA composite. More  
303 importantly, the GO films covering the surface of the EP/PA composite can greatly prevent the  
304 leakage problems of molten paraffin. No leakage of paraffin occurred after thermal cycling 3000  
305 times. Therefore, the EP/PA/GO composites have shown a great potential for thermal energy  
306 storage applications due to the enhanced thermal properties, good leakage-bearing properties and  
307 excellent chemical compatibility.

308

#### 309 Acknowledgements

310 The authors would like to acknowledge the financial support from the Hong Kong Research  
311 Grant Council under the Grant 615810, the China Ministry of Science and Technology under the  
312 Grant 2015CB655100, Information Technology of Guangzhou under the Grant 2013J4500069  
313 and the Natural Science Foundation of China under the Grant 51302104.

314

#### 315 References

- 316 [1] Kalogirou SA, Florides G, Tassou S. Energy analysis of buildings employing thermal  
317 mass in Cyprus. *Renewable Energy*. 2002;27(3):353-68.
- 318 [2] Bojić M, Miletić M, Bojić L. Optimization of thermal insulation to achieve energy  
319 savings in low energy house (refurbishment). *Energy Conversion and Management*.  
320 2014;84:681-90.
- 321 [3] Kalogirou SA, Karellas S, Badescu V, Braimakis K. Exergy analysis on solar thermal  
322 systems: A better understanding of their sustainability. *Renewable Energy*. 2015.
- 323 [4] Şahan N, Fois M, Paksoy H. Improving thermal conductivity phase change materials—A  
324 study of paraffin nanomagnetite composites. *Solar Energy Materials and Solar Cells*.  
325 2015;137:61-7.
- 326 [5] Kalogirou SA. Solar thermal collectors and applications. *Progress in energy and*  
327 *combustion science*. 2004;30(3):231-95.

- 328 [6] Song S, Dong L, Zhang Y, Chen S, Li Q, Guo Y, et al. Lauric acid/intercalated kaolinite  
329 as form-stable phase change material for thermal energy storage. *Energy*. 2014;76:385-9.
- 330 [7] Chung O, Jeong S-G, Kim S. Preparation of energy efficient paraffinic PCMs/expanded  
331 vermiculite and perlite composites for energy saving in buildings. *Solar Energy Materials and*  
332 *Solar Cells*. 2015;137:107-12.
- 333 [8] Zhang Y, Zheng X, Wang H, Du Q. Encapsulated phase change materials stabilized by  
334 modified graphene oxide. *Journal of Materials Chemistry A*. 2014;2(15):5304-14.
- 335 [9] Chen Z, Wang J, Yu F, Zhang Z, Gao X. Preparation and properties of graphene oxide-  
336 modified poly (melamine-formaldehyde) microcapsules containing phase change material n-  
337 dodecanol for thermal energy storage. *Journal of Materials Chemistry A*. 2015;3(21):11624-30.
- 338 [10] Fu X, Liu Z, Xiao Y, Wang J, Lei J. Preparation and properties of lauric acid/diatomite  
339 composites as novel form-stable phase change materials for thermal energy storage. *Energy and*  
340 *Buildings*. 2015.
- 341 [11] Li X, Sanjayan JG, Wilson JL. Fabrication and stability of form-stable diatomite/paraffin  
342 phase change material composites. *Energy and Buildings*. 2014;76:284-94.
- 343 [12] Zhang J, Guan X, Song X, Hou H, Yang Z, Zhu J. Preparation and properties of gypsum  
344 based energy storage materials with capric acid–palmitic acid/expanded perlite composite PCM.  
345 *Energy and Buildings*. 2015;92:155-60.
- 346 [13] Lu Z, Xu B, Zhang J, Zhu Y, Sun G, Li Z. Preparation and characterization of expanded  
347 perlite/paraffin composite as form-stable phase change material. *Solar Energy*. 2014;108:460-6.
- 348 [14] Lu Z, Zhang J, Sun G, Xu B, Li Z, Gong C. Effects of the form-stable expanded  
349 perlite/paraffin composite on cement manufactured by extrusion technique. *Energy*. 2015.
- 350 [15] Yuan Y, Yuan Y, Zhang N, Du Y, Cao X. Preparation and thermal characterization of  
351 capric–myristic–palmitic acid/expanded graphite composite as phase change material for energy  
352 storage. *Materials Letters*. 2014;125:154-7.
- 353 [16] Wang S, Qin P, Fang X, Zhang Z, Wang S, Liu X. A novel sebacic acid/expanded graphite  
354 composite phase change material for solar thermal medium-temperature applications. *Solar*  
355 *Energy*. 2014;99:283-90.
- 356 [17] Tian H, Wang W, Ding J, Wei X, Song M, Yang J. Thermal conductivities and  
357 characteristics of ternary eutectic chloride/expanded graphite thermal energy storage composites.  
358 *Applied Energy*. 2015;148:87-92.
- 359 [18] Mhike W, Focke WW, Mofokeng J, Luyt AS. Thermally conductive phase-change  
360 materials for energy storage based on low-density polyethylene, soft Fischer–Tropsch wax and  
361 graphite. *Thermochimica Acta*. 2012;527:75-82.
- 362 [19] Xu B, Li Z. Paraffin/diatomite/multi-wall carbon nanotubes composite phase change  
363 material tailor-made for thermal energy storage cement-based composites. *Energy*. 2014;72:371-  
364 80.
- 365 [20] Ramadoss A, Saravanakumar B, Kim SJ. Thermally Reduced Graphene Oxide-coated  
366 Fabrics for Flexible Supercapacitors and Self-powered Systems. *Nano Energy*. 2015.
- 367 [21] Wang Z, Liu C-J. Preparation and application of iron oxide/graphene based composites  
368 for electrochemical energy storage and energy conversion devices: Current status and  
369 perspective. *Nano Energy*. 2015;11:277-93.
- 370 [22] Yang H, Lee D, Park K, Kim W. Platinum–boron doped graphene intercalated by carbon  
371 black for cathode catalyst in proton exchange membrane fuel cell. *Energy*. 2015.
- 372 [23] Tsetseris L, Pantelides S. Graphene: An impermeable or selectively permeable membrane  
373 for atomic species? *Carbon*. 2014;67:58-63.

- 374 [24] Hummers Jr WS, Offeman RE. Preparation of graphitic oxide. Journal of the American  
375 Chemical Society. 1958;80(6):1339-.
- 376 [25] Liu C, Yuan Y, Zhang N, Cao X, Yang X. A novel PCM of lauric–myristic–stearic  
377 acid/expanded graphite composite for thermal energy storage. Materials Letters. 2014;120:43-6.  
378

## Figures Captions

**Fig. 1.** Image of the EP/PA composite and the EP/PA/GO0.5 composite.

**Fig. 2.** DSC curves of the EP/PA composite with different GO contents.

**Fig. 3.** TGA curves of the EP/PA composite with different GO contents.

**Fig. 4.** Schematic diagram of heat storage/release performance test.

**Fig. 5.** Melting (a) and freezing (b) curves of the EP/PA composite, the EP/PA/GO0.25 composite and the EP/PA/GO0.5 composite.

**Fig. 6.** FTIR curves of the GO, EP/PA composite and EP/PA/GO0.5 composite.

**Fig. 7.** The surface morphologies of (a) the expanded perlite, (b) the EP/PA composite and (c) the EP/PA/GO0.5 composite.

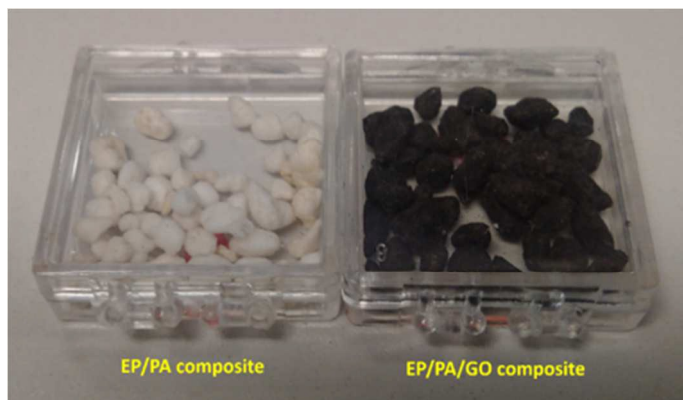
**Fig. 8.** Leakage test for the GO films.

**Fig. 9.** Thermal cycling test.

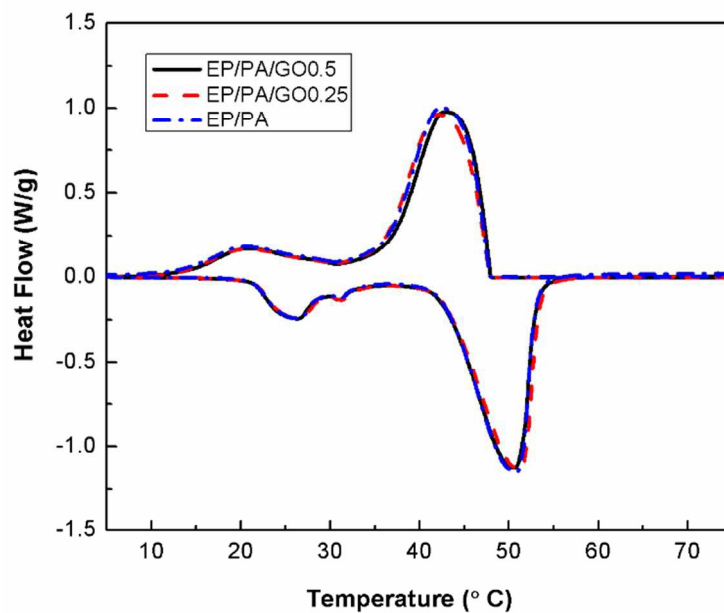
**Fig. 10.** Leakage test for the EP/PA composite (a) before thermal cycling test (b) after 1500 cycling (c) after 3000 cycling; the EP/PA/GO0.5 composite (d) before thermal cycling test (e) after 1500 cycling (f) after 3000 cycling.

**Fig. 11.** (a) Cross-section image of the EP/PA/GO0.5 composite; (b) XPS spectra of the GO.

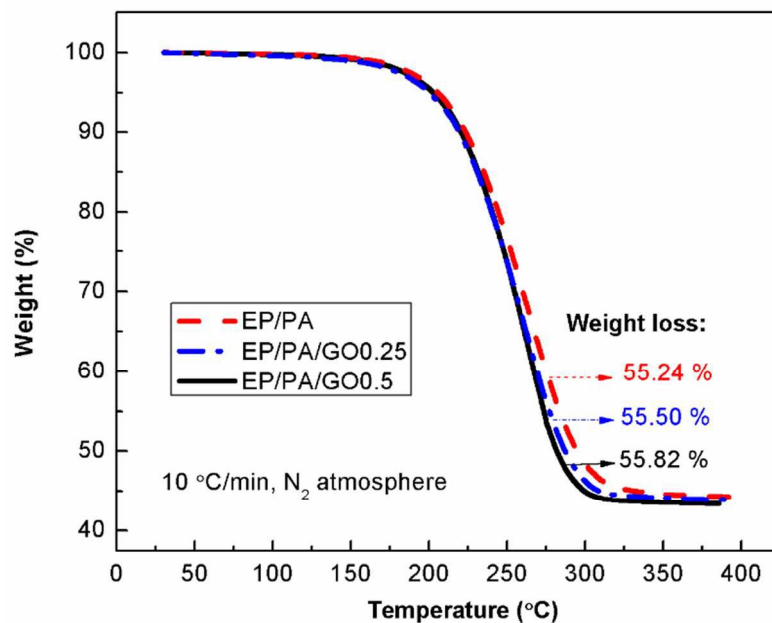
## Figures



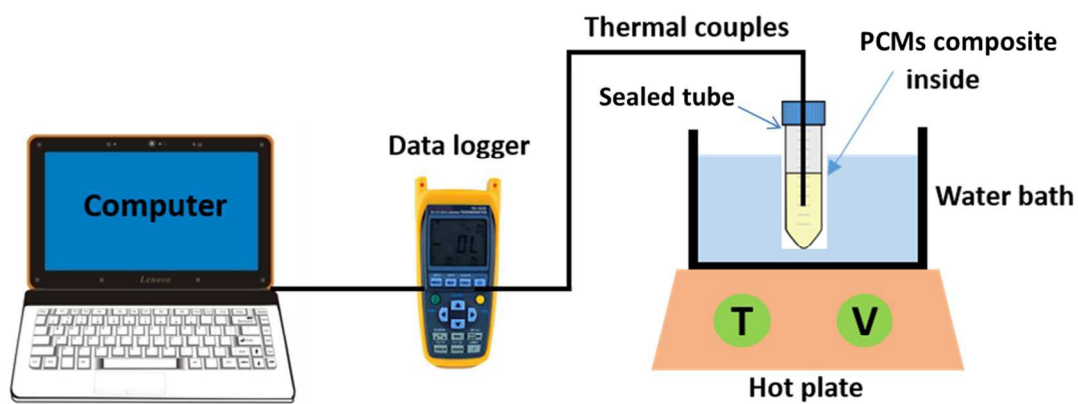
**Fig. 1.** Image of the EP/PA composite and the EP/PA/GO0.5 composite.



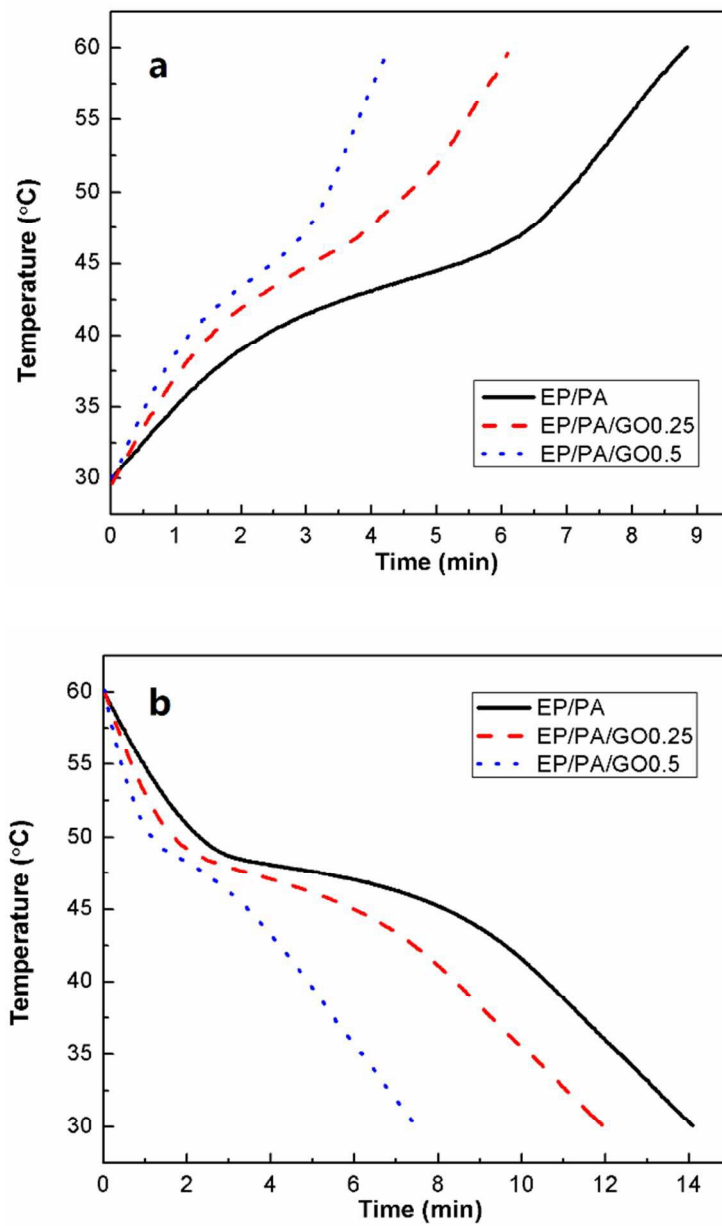
**Fig. 2.** DSC curves of the EP/PA composite with different GO contents.



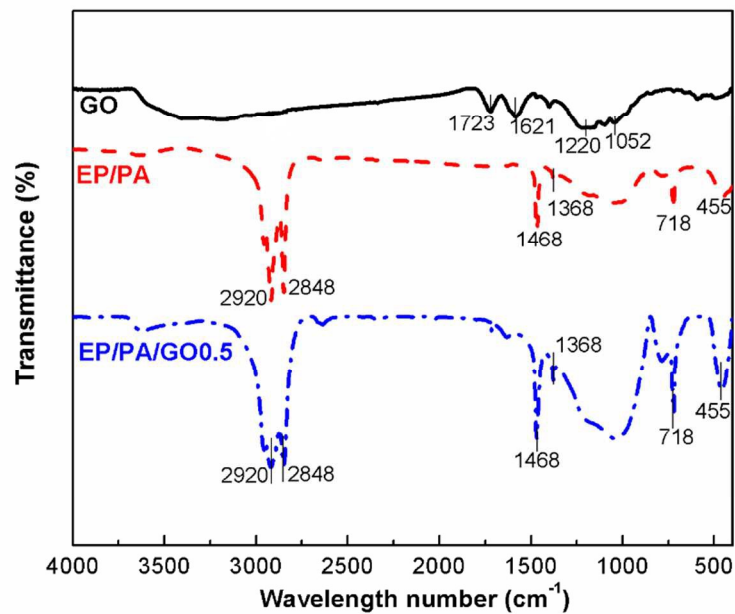
**Fig. 3.** TGA curves of the EP/PA composite with different GO contents.



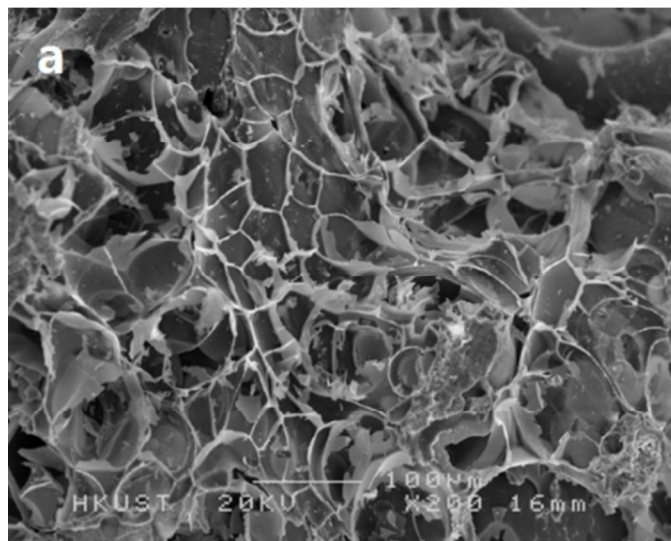
**Fig. 4.** Schematic diagram of heat storage/release performance test.



**Fig. 5.** Melting (a) and freezing (b) curves of the EP/PA composite, the EP/PA/GO0.25 composite and the EP/PA/GO0.5 composite.



**Fig. 6.** FTIR curves of the GO, EP/PA composite and EP/PA/GO0.5 composite.



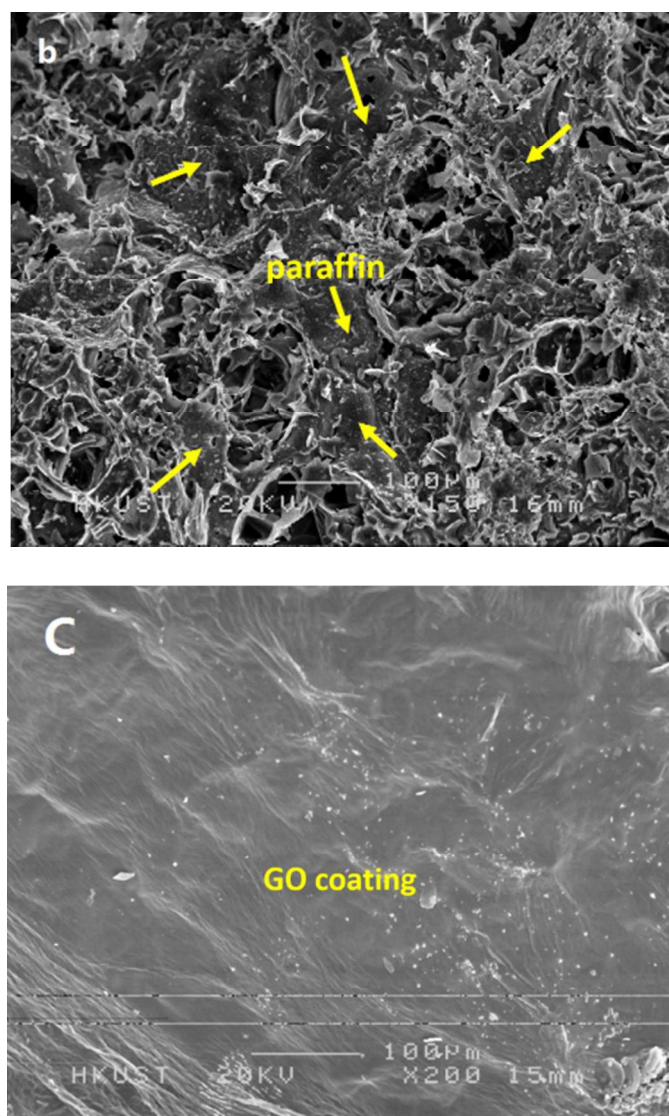


**Fig. 7.** The surface morphologies of (a) the expanded perlite, (b) the EP/PA composite and (c) the EP/PA/GO0.5 composite.

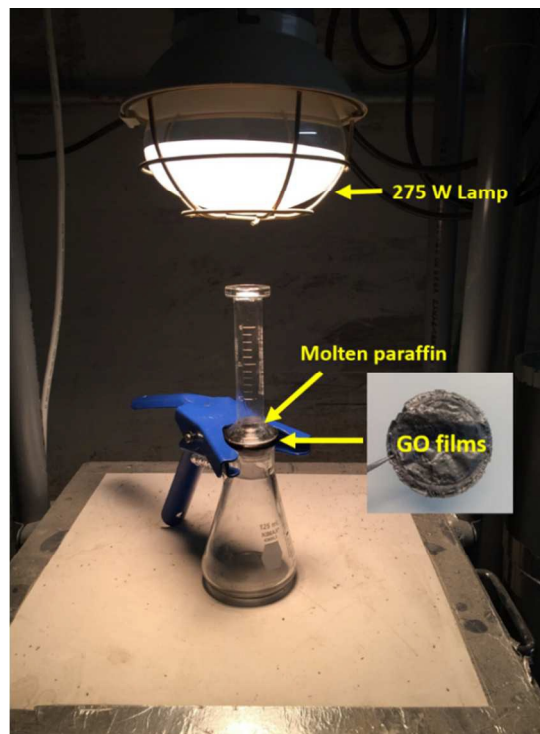


**Fig. 8.** Leakage test for the GO films.

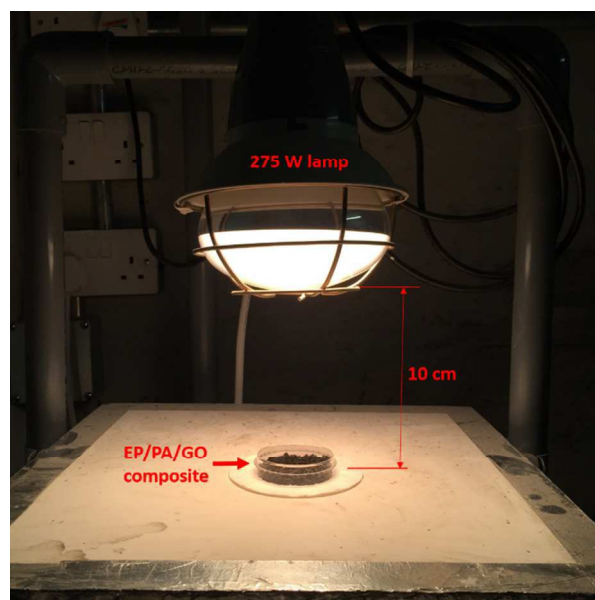


**Fig. 9.** Thermal cycling test.

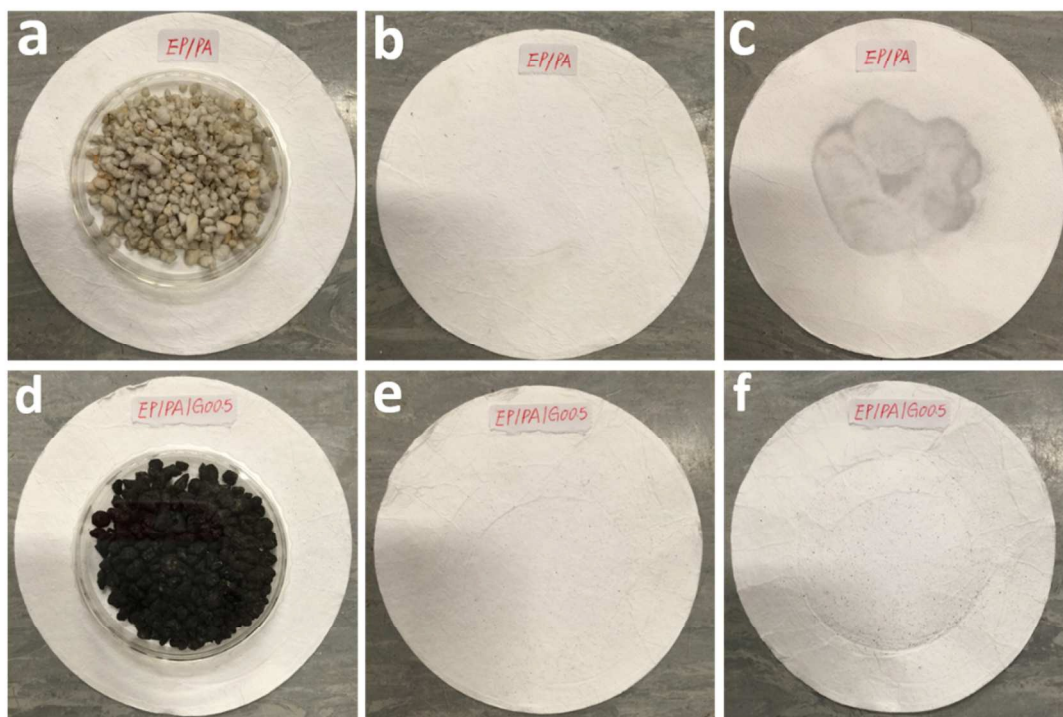


**Fig. 10.** Leakage test for the EP/PA composite (a) before thermal cycling test (b) after 1500 cycling (c) after 3000 cycling; the EP/PA/GO0.5 composite (d) before thermal cycling test (e) after 1500 cycling (f) after 3000 cycling.

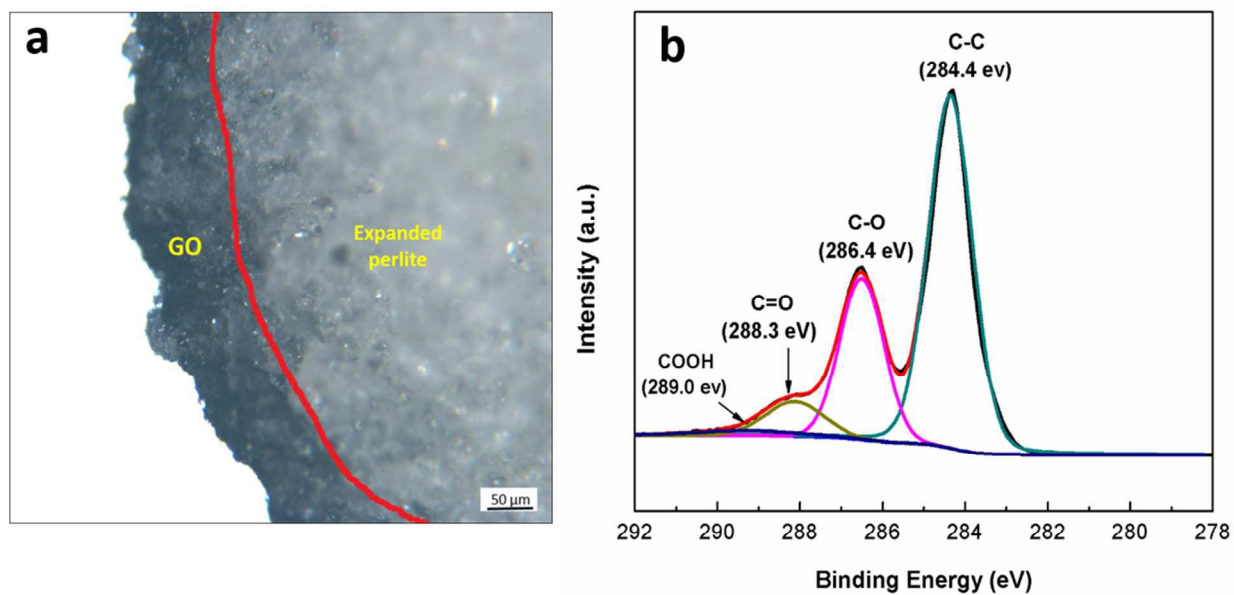


**Fig. 11.** (a) Cross-sectional image of the EP/PA/GO0.5 composite; (b) XPS spectra of the GO.